Periodica Polytechnica
Mechanical Engineering

60(2), pp. 113-120, 2016
DOI: 10.3311/PPme.8734


# Numerical Modeling of an FG Plate Behavior Impacted at Low Velocity in a Temperature Field

Amine Smahat[1], Abdelkader Megueni[1*]

RESEARCH ARTICLE

Received 29 October 2015; accepted after revision 19 January 2016

***Abstract***

*This paper analyzes the behavior of a functionnally graded plate subjected to impact force at a low velocity by adopting the Hertz law. The differential equation which governs the impact phenomenon is used to calculate the contact force, indentation and indentation velocity. Elastic properties of the FGM plate are obtained by integration of the components volume fraction across the thickness. A parametric study is conducted to evaluate effects of temperature, the power law index, the projectile mass on the contact force and indentation. The results obtained are compared to those in the literature for other structures.*

***Keywords***

*FGM plate, impact, contact force, indentation, temperature, velocity, index*

[1] Laboratory of Structures and Solids Mechanics (LMSS), Faculty of Technology, University Djilali Liabes of Sidi Bel Abbès (22000), Algeria

[*] Corresponding author, e-mail: a_megueni@yahoo.fr

## 1 Introduction

Composite materials are widely used in various fields of mechanical engineering (automotive, aeronautics, aerospace, etc ...) and often subjected to impact loads. Abrate [1] has modeled the impact phenomenon by studying the response of a composite plate impacted at low velocity. It uses energy-balance models to assess the strength and the contact time. Many authors are interested in the study of the behavior of structures subjected to impact loads [2-6]. Larson et al. [5, 6] developed a combined analytical and experimental methods to study the behavior of a Functionnally graded circular plate under different boundary conditions. Different approaches are used to modelize the impact phenomenon. Olsson [7] modeled the impact using an approach to study an infinite composite plate. Kiani et al. [8] was interested in the study of FGM thick beams in thermal field by the finite element method. Mao et al. [9] investigated the response of a recessed spherical shell FGM by applying the Galerkin method. Qian and Swanson [10] studied the comparison of the technical solutions of the response of a composite plate. Boroujerdy and Kiani [14] were interested in the dynamic behaviour of a composite laminated beam subjected to multiple projectiles under high temperature field. Jam and Kiani [15] analyzed the response of functionally graded carbon nanotube reinforced composite (FG-CNTRC) beam subjected to the action of an impacting mass.

The materials properties of Functionnally graded materials (FGM) are recent advanced composite materials, developed by a group of Japanese scientists in 1980. They used as a thermal barrier and allow the removal of thermal residual stresses.

Functionally graded materials have significant advantages over traditional materials. They consist of two materials, generally ceramic and metal, the volume fraction of one varies according to one or more directions with a determined law (power, exponential, ... etc.).

Studies on the modeling of the response of the FGM structure subjected to low velocity impact forces are almost rare.

Our study is to analyze the response of an FGM plate impacted at low speed by combining two approaches. We use the differential equation developed by Ollsson [7] which governs the

behavior of an infinite impacted composite plate. In the case of an FGM plate, our approach is to use the modeling of FGM proposed by Efraim [11]. The study was made under different temperatures by varying the proportion of FGM constituents.

## 2 Problem formulation

### 2.1 Model description

Olsson [7] modeled the impact of a projectile over an infinite plate of composite materials at low speed by a differential equation of order 2 obtained by using the following Hertz law:

$F = k_c \bar{\alpha}^{3/2}$, $k_c$ is the contact stiffness

The indentation is obtained by solving the differential equation [7]:

$$\frac{d^2\bar{\alpha}}{d\bar{t}^2} + \lambda \frac{3}{2} \bar{\alpha}^{1/2} \frac{d\bar{\alpha}}{d\bar{t}} + \bar{\alpha}^{3/2} = 0 \tag{1}$$

With the initial conditions $\bar{\alpha}(0) = 0$, $\frac{d(\bar{\alpha})}{d\bar{t}} = 0$

Which nondimensionnel indentation and time are:

$$\bar{\alpha} = \frac{\alpha}{TV}, \bar{t} = \frac{t}{T}$$

Where:

$$T = \left[ M / \left( k_c V^{1/2} \right) \right]^{2/5} \tag{2}$$

$V$, $M$ represent respectively projectile velocity and mass.

$T$ is the contact time of the projectile with the plate

$\lambda$ is a dimensionless parameter defined by:

$$\lambda = k_c^{2/5} V^{1/5} M^{3/5} / \left[ 8\sqrt{\bar{m}D} \right] \tag{3}$$

$\bar{m}$ is the average of the plate density

$k_c$ and $D$ respectively express the contact stiffness and bending

$$k_c = \frac{4}{3} E\sqrt{R} \quad \text{and} \quad D = \frac{Eh^3}{12\left(1-\nu^2\right)} \tag{4}$$

$R$ (the projectile radius) and $E$ are respectively calculated by the following expressions:

$$\frac{1}{R} = \frac{1}{R_1} + \frac{1}{R_2}, \quad \frac{1}{E} = \frac{1-\nu_1^2}{E_1} + \frac{1-\nu_2^2}{E_2} \tag{5}$$

$R_1$, $R_2$ are radius of curvature of respectively the plate and the projectile. $E_1$, $E_2$, $\nu_1$, $\nu_2$ are respectively elastic properties (Young's modulus, Poisson's ratio) of these two materials.

The contact force is expressed by:

$$P = \left[ k^2 M^3 V^6 \right]^{1/5} \bar{\alpha}^{3/2}. \tag{6}$$

### 2.2 Modeling the FGM material

We are interested in the study of an FGM plate impacted by a low velocity spherical projectile in a temperature field. The volume fraction of the components varies according to the plate thickness $h$ using to the following law (power law).

$$V_{m,c=} \left( \frac{2z+h}{2h} \right)^n \tag{7}$$

The thermal and mechanical properties (Young's modulus, Poisson coefficient, thermal conductivity, thermal expansion coefficient) vary according to the temperature using the nonlinear function [12]:

$$P_j = p_0 \left( p_{-1} T^{-1} + 1 + p_1 T + p_2 T^2 + p_3 T^3 \right) \tag{8}$$

Where:

$p_0$, $p_1$, $p_1$, $p_2$ and $p_3$ are temperature coefficients (in Kelvin). Typical values for mechanical and thermal properties (ceramic, metal) are presented in Table 1 [13].

While the elastic and physical properties are given by:

$$\begin{aligned} E_{FGM}(Z,T) &= \left[ E_m(T) - E_c(T) \right] \left( \frac{2z+h}{2h} \right)^n + E_c(T) \\ \nu_{FGM}(Z,T) &= \left[ \nu_m(T) - \nu_c(T) \right] \left( \frac{2z+h}{2h} \right)^n + \nu_c(T) \\ \rho_{FGM}(Z,T) &= \left[ \rho_m(T) - \rho_c(T) \right] \left( \frac{2z+h}{2h} \right)^n + \rho_c(T) \end{aligned} \tag{9}$$

The modeling of FGM used by Efraim [11] is obtained by integration of the metal, and ceramics volume fractions through the plate thickness as.

**Table 1** Temperature dependent coefficients for ceramic and metal.

| Materials | Property | $P_0$ | $P_{-1}$ | $P_1$ | $P_2$ | $P_3$ |
|---|---|---|---|---|---|---|
| Nickel | E (Pa) | 223.95e 9 | 0 | -2.794e -4 | -3.998e -9 | 0 |
| | α (1/K) | 9.9209e -6 | 0 | 8.705e -4 | 0 | 0 |
| | ρ (kg/m$^3$) | 8902 | 0 | 0 | 0 | 0 |
| | ν | 0.31 | 0 | 0 | 0 | 0 |
| Aluminium oxide | E (Pa) | 349.55e 9 | 0 | -3.853e-4 | 4.027e -7 | -1.673e -10 |
| | α (1/K) | 6.8269e -6 | 0 | 1.838e-4 | 0 | 0 |
| | ρ (kg/m$^3$) | 3950 | 0 | 0 | 0 | 0 |
| | ν | 0.26 | 0 | 0 | 0 | 0 |

$$V_c = \frac{1}{h}\int_{-h/2}^{h/2}\left(\frac{1}{2}+\frac{z}{h}\right)^n dz = \frac{1}{1+n} \tag{10}$$

$$V_m = 1 - V_c = \frac{n}{1+n} \tag{11}$$

Hence elastic expressions and physical properties of the modeled FGM:

$$\begin{aligned} E_{FGM}(Z,T) &= E_m(T)V_m + E_c(T)V_c \\ \nu_{FGM}(Z,T) &= \nu_m(T)V_m + \nu_c(T)V_c \\ \rho_{FGM}(Z,T) &= \rho_m(T)V_m - \rho_c(T)V_c \end{aligned} \tag{12}$$

## 3 Results and discussions

Consider a ceramic -metal plate type Ni-$Al_2O_3$ of thickness $h$ = 5 mm which the phases of the mechanical properties are reported in Table 1. It is impacted by a spherical projectile of radius $R$ = 6.35 mm steel, of mass $m$ = 8.3537 g, of Young's modulus $E$ = 200 000 MPa, and a velocity equal to 3.0 m/s. The resolution of the differential Eq. (1) is made in Matlab. We calculate the dimensionless indentation $\bar{\alpha}$ and the corresponding velocity and deduce the $\alpha$ indentation. The contact force is deduced from the Eq. (6).

Figures 1-3 show the variation of the contact force, indentation and indentation speed according to the time for a volume fraction index of $n$ = 0 at different temperatures. Maximum contact is noted in Fig. 1 that the rigidity and the strength decreases when the temperature increases (Table 2) and the opposite effect is observed for contact time while Fig. 2 shows that the indentation increases with increase in temperature. Figure 3 shows the variation of the indentation velocity over time. This figure shows two zones, a downward linear portion in the time interval [0-2.5 μs] and a constant part approximately equal to 0.4 m/s. The same behavior of the contact force, indentation and indentation velocity is observed in Figs. 4-9 respectively for volume fraction index $n$ = 2 and $n$ = 10 (Tables 3, 4). Figures 10-12 show the variation of the contact force, indentation and indentation velocity over time to a temperature T = 20 °C at different indexes n of volume fraction. Figure 10 shows that the maximum contact force increases with the increase of the index $n$ (Table 3) and the opposite effect is observed for the contact time.

**Table 2** Inelastic parameter, contact stiffness and contact forces as a function of the temperature ($n$ = 0)

| Temperature (Kelvin) | $\lambda$ | $k_c$ (N/m) | $F_{max}$ (N) |
|---|---|---|---|
| 273 | 0.4450 | 1.2040 e+10 | 1.8015 e+3 |
| 573 | 0.4578 | 1.1473 e+10 | 1.7510 e+3 |
| 973 | 0.4768 | 1.0626 e+10 | 1.6753 e+3 |

**Table 3** Inelastic parameter, contact stiffness and contact forces as a function of the temperature ($n$ = 2)

| Temperature (Kelvin) | $\lambda$ | $k_c$ (N/m) | $F_{max}$ (N) |
|---|---|---|---|
| 273 | 0.2982 | 1.3650 e+10 | 2.1168 e+3 |
| 573 | 0.3107 | 1.2901 e+10 | 2.0486 e+3 |
| 973 | 0.3304 | 1.1711 e+10 | 1.9393 e+3 |

**Table 4** Inelastic parameter, contact stiffness and contact forces as a function of the temperature ($n$ = 10)

| Temperature (Kelvin) | $\lambda$ | $k_c$ (N/m) | $F_{max}$ (N) |
|---|---|---|---|
| 273 | 0.2679 | 1.4123 e+10 | 2.1998 e+3 |
| 573 | 0.2802 | 1.3333 e+10 | 2.1281 e+3 |
| 973 | 0.2997 | 1.2056 e+10 | 2.0118 e+3 |

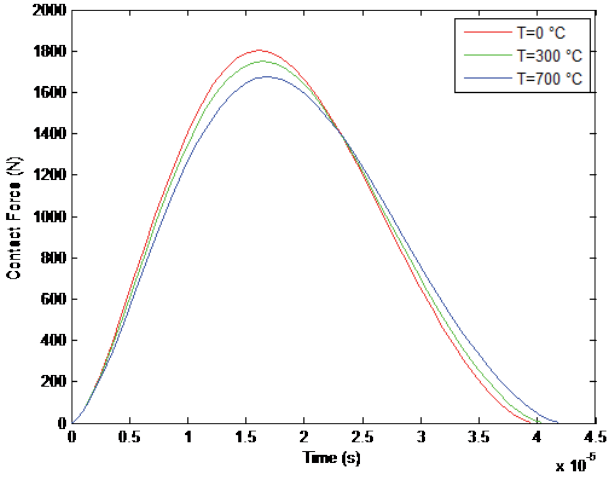


**Fig. 1** Effect of temperature on contact force in FGM plate ($n$ = 0)

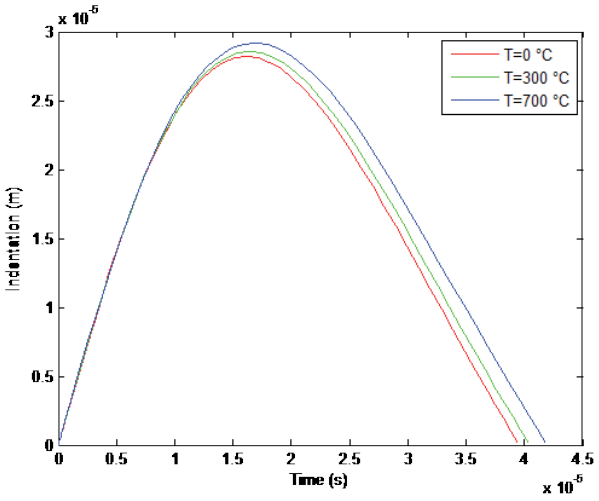


**Fig. 2** Effect of temperature on indentation in FGM plate ($n$ = 0)

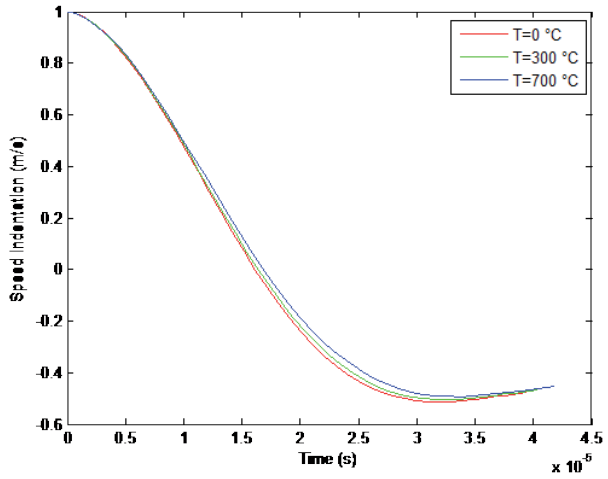


**Fig. 3** Effect of temperature on indentation velocity of FGM plate ($n = 0$)

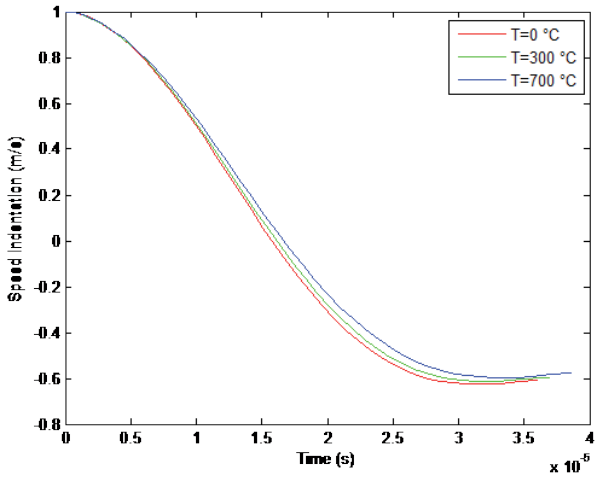


**Fig. 6** Effect of temperature on indentation velocity of FGM plate ($n = 2$)

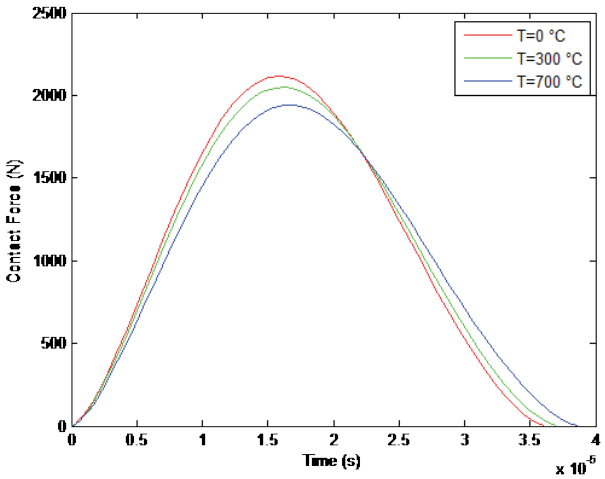


**Fig. 4** Effect of temperature on contact force in FGM plate ($n = 2$)

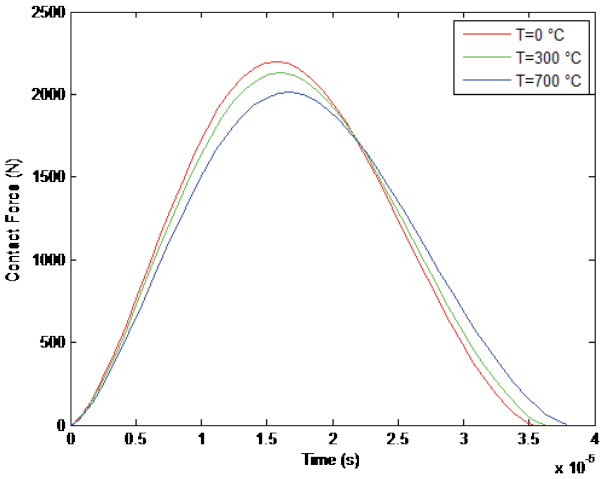


**Fig. 7** Effect of temperature on contact force in FGM plate ($n = 10$)

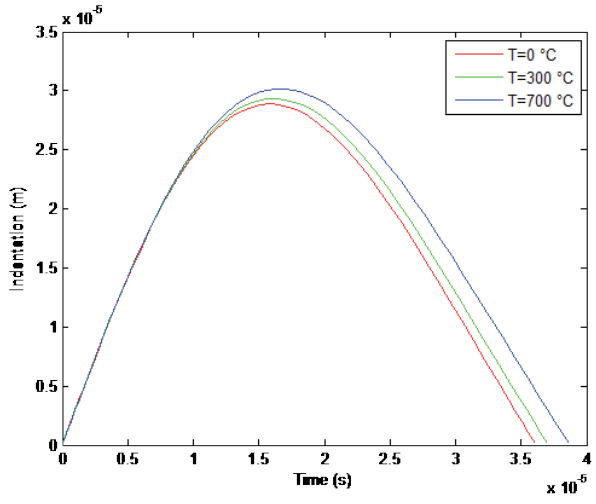


**Fig. 5** Effect of temperature on indentation in FGM plate ($n = 2$)

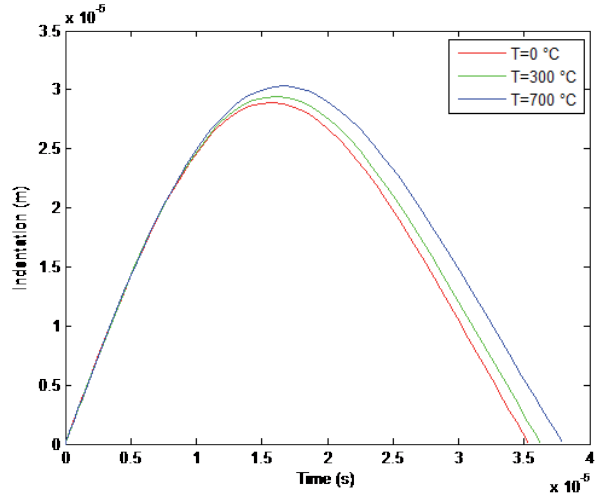


**Fig. 8** Effect of temperature on indentation in FGM plate ($n = 10$)

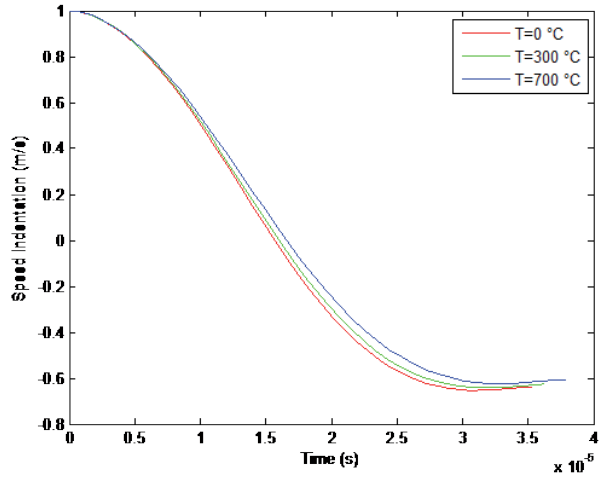


**Fig. 9** Effect of temperature on indentation velocity of FGM plate ($n$ = 10)

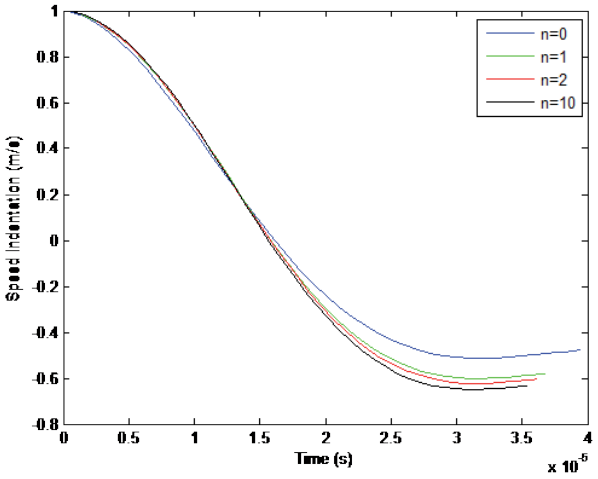


**Fig. 12** Effect of power law index on indentation velocity of FGM plate (T = 20 °C)

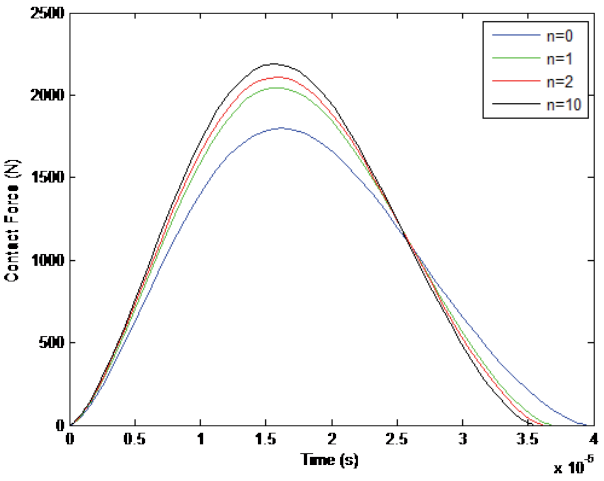


**Fig. 10** Effect of power law index on contact force in FGM plate (T = 20 °C)

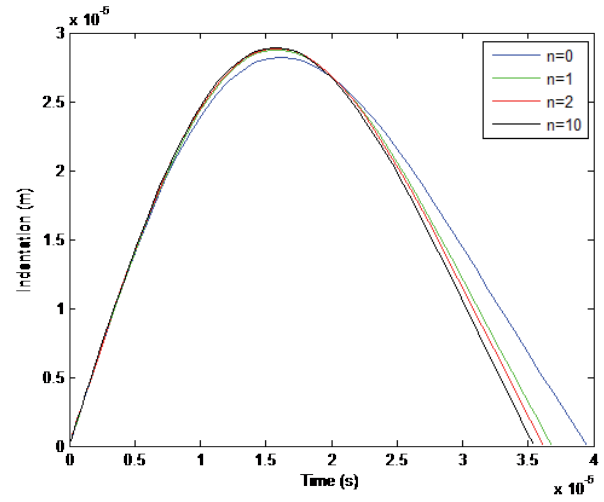


**Fig. 11** Effect of power law index on indentation in FGM plate (T = 20 °C)

Figures 13-15 represent the same curves as those presented in Figs. 10-12 for a temperature T = 300 °C where it is observed the same behavior of the maximum values of contact force and indentation.

Figures 16-18 also show the same curves as shown in Figures 10-15 for a temperature T = 700 °C where the same behavior is observed.

The maximum contact forces, corresponding indentations decrease with increasing temperature (Table 5-7).

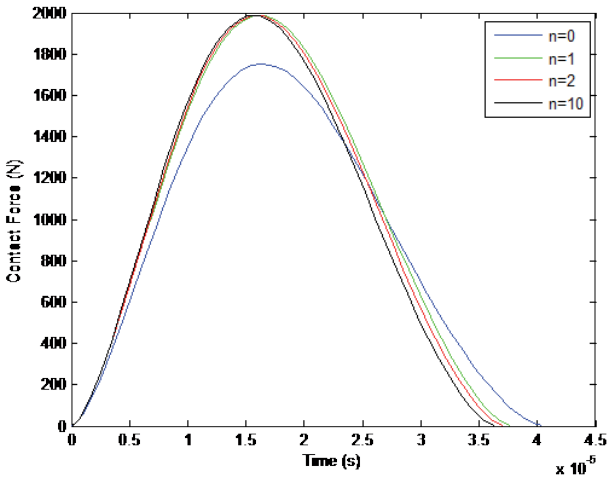


**Fig. 13** Effect of power law index on contact force in FGM plate (T = 300 °C)

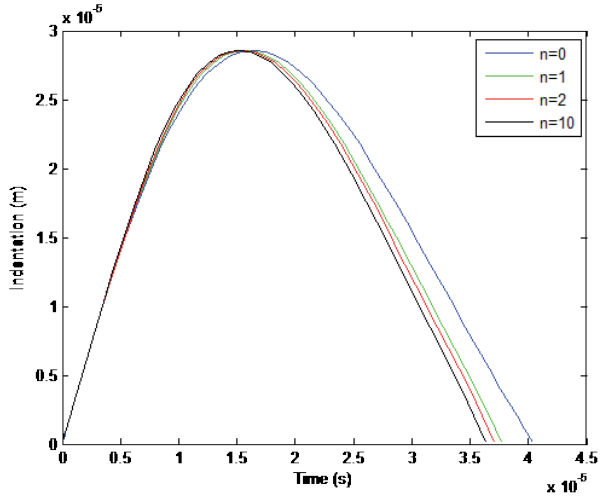


**Fig. 14** Effect of power law index on indentation in FGM plate (T = 300 °C)

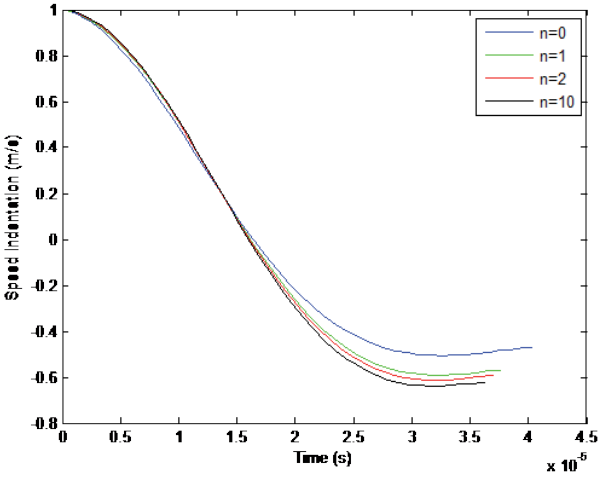


**Fig. 15** Effect of power law index on indentation velocity of FGM plate (T = 300 °C)

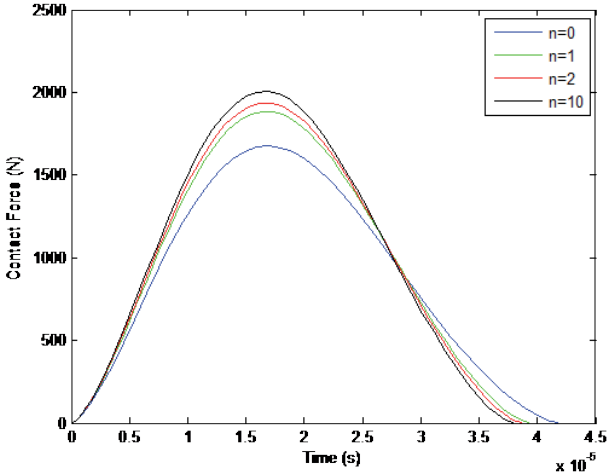


**Fig. 16** Effect of power law index on contact force in FGM plate (T = 700 °C)

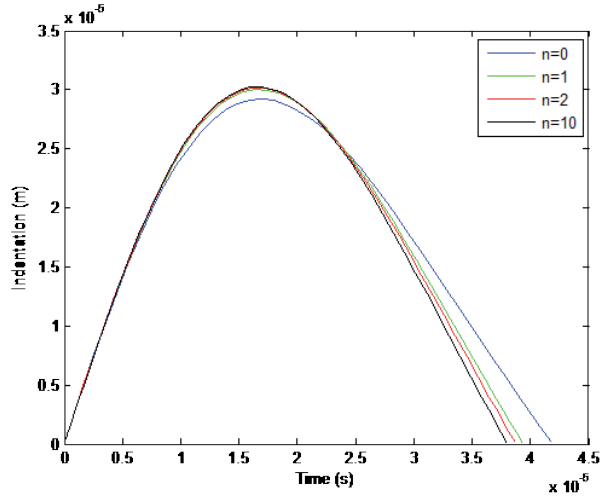


**Fig. 17** Effect of power law index on indentation in FGM plate (T = 700 °C)

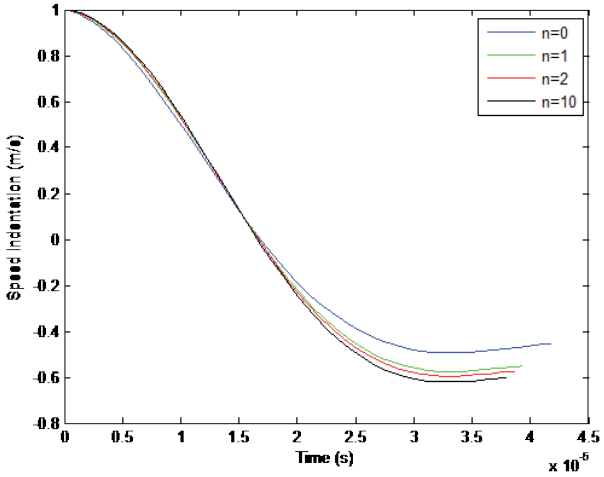


**Fig. 18** Effect of power law index on indentation velocity of FGM plate (T = 700 °C)

**Table 5** Inelastic parameter, contact stiffness and contact forces as a function of the temperature ($n$ = 10)

| $n$ | $\lambda$ | $k_c$ (N/m) | $F_{max}$ (N) |
|---|---|---|---|
| 0 | 0.4443 | 1.2003e+10 | 1.8002e+03 |
| 1 | 0.3263 | 1.3250e+10 | 2.0441e+03 |
| 2 | 0.3012 | 1.3604e+10 | 2.1086e+03 |
| 10 | 0.2716 | 1.4074e+10 | 2.1901e+03 |

**Table 6** Inelastic parameter, contact stiffness and contact forces as a function of $n$ (T = 300 °C)

| $n$ | $\lambda$ | $k_c$ (N/m) | $F_{max}$ (N) |
|---|---|---|---|
| 0 | 0.4563 | 1.1473e+10 | 1.7528e+03 |
| 1 | 0.3382 | 1.2580e+10 | 1.9835e+03 |
| 2 | 0.3130 | 1.2901e+10 | 2.0444e+03 |
| 10 | 0.2832 | 1.3333e+10 | 2.1229e+03 |

**Table 7** Inelastic parameter, contact stiffness and contact forces as a function of $n$ (T = 700 °C)

| $n$ | $\lambda$ | $k_c$ (N/m) | $F_{max}$ (N) |
|---|---|---|---|
| 0 | 0.4752 | 1.0626e+10 | 1.6771e+03 |
| 1 | 0.3579 | 1.1460e+10 | 1.8832e+03 |
| 2 | 0.3328 | 1.1711e+10 | 1.9356e+03 |
| 10 | 0.3030 | 1.2056e+10 | 2.0062e+03 |

The effect of the plate thickness is significant. The maximum force passes from 800 to 2600 N when the thickness varies from 2 mm to 10 mm at T = 25 °C for an index $n$ = 2 (Fig. 19). Figure 20 shows this effect on the indentation. Figure 21 also shows this effect, for a thin thikhness, the constant part of the indentationvelocity tend towards zero.

The increase of mass increases the maximum contact force, indentation and the contact time (Figs. 22-24).

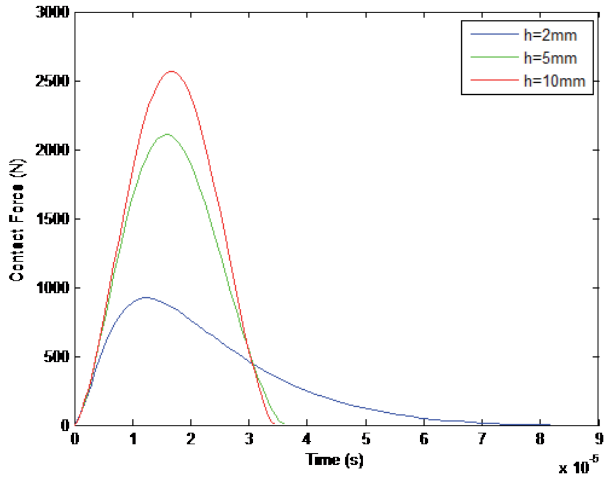


**Fig. 19** Effect of plate thickness on contact force (T = 25 °C, $n$ = 2)

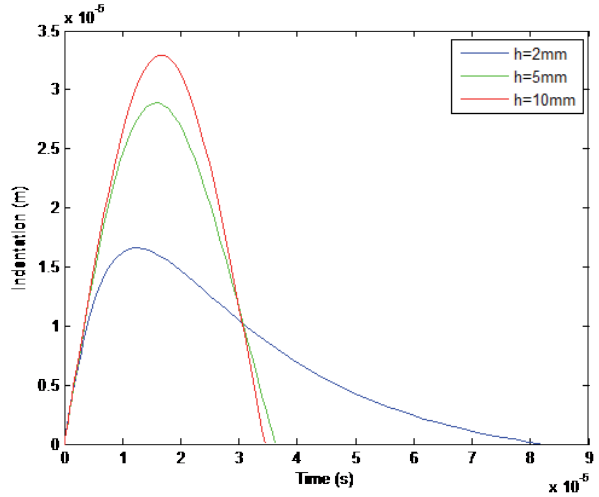


**Fig. 20** Effect of plate thickness on indentation (T = 25 °C, $n$ = 2)

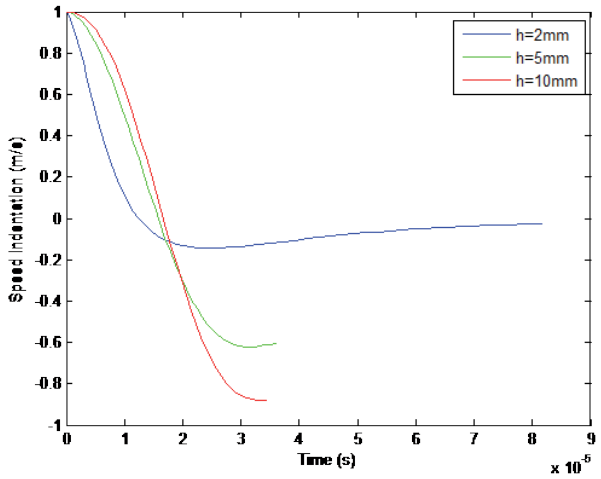


**Fig. 21** Effect of plate thickness on indentation velocity (T = 25 °C, $n$ = 2)

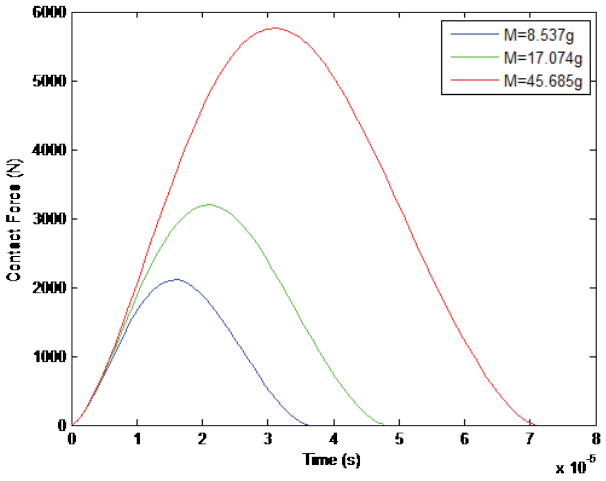


**Fig. 22** Effect of projectile mass on contact force (T = 25 °C, $n$ = 2)

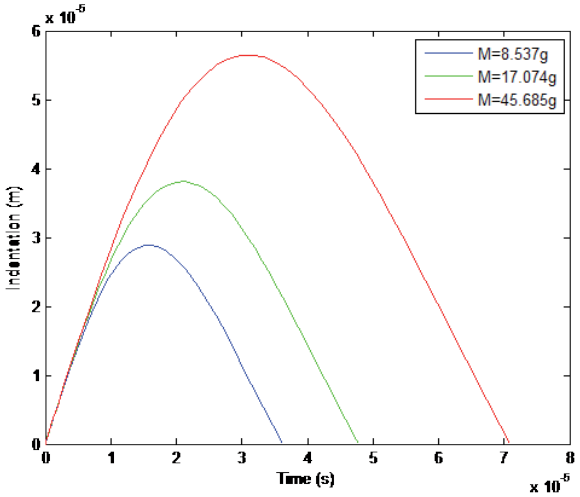


**Fig. 23** Effect of projectile mass on indentation (T = 25 °C, $n$ = 2)

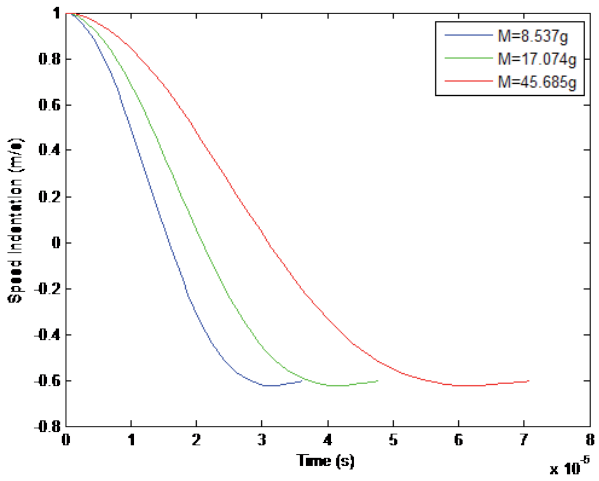


**Fig. 24** Effect of projectile mass on indentation velocity (T = 25 °C, $n$ = 2)

## 4 Conclusions

This work permits us to deduce the following conclusions.

Using an integration of FGM modeled by volume fraction depending on the thickness and application of Ollson model for a plate impacted at low velocity allows us to make the following conclusions:

1. The minimum of the maximum contact force is obtained for a ceramic ($n$ = 0) and a high temperature T = 700 °C.
2. The minimum of the maximum indentation is also obtained for a ceramic at the same temperature (T = 700 °C). It is in the range of 2.9204e-5
3. A small plate thickness significantly reduces the maximum contact force and indentation
4. The mass of the projectile has a significant negative effect on the contact force and indentation and lengthens the contact time.

## References

[1] Abrate, S. "Modeling of impacts on composite structures." *Composite Structures*. 51(2), pp. 129-138. 2001. DOI: 10.1016/S0263-8223(00)00138-0

[2] Gunes, R., Aydin, M. "Elastic response of functionally graded circular plates under a drop-weight." *Composite Structures*. 92(10), pp. 2445-2456. 2010. DOI: 10.1016/j.compstruct.2010.02.015

[3] Gunes, R., Aydin, M., Apalak, M. K., Reddy, J. N. "The elasto-plastic impact analysis of functionally graded circular plates under low-velocities original research article." *Composite Structures*. 93(2), pp. 860-869. 2011. DOI: 10.1016/j.compstruct.2010.07.008

[4] Etemadi, E., Afaghi Khatibi, A., Takaffoli, M. "3D finite element simulation of sandwich panels with a functionally graded core subjected to low velocity impact." *Composite Structures*. 89(1), pp. 28-34. 2009. DOI: 10.1016/j.compstruct.2008.06.013

[5] Larson, R. A., Palazotto, A. N., Gardenier, H. E. "Impact response of titanium and titanium boride monolithic and functionally graded composite plates." *AIAA Journal*. 47(3), pp. 676-691. 2009. DOI: 10.2514/1.38577

[6] Larson, R. A., Palazotto, A. N. "Property estimation in FGM plates subjected to low velocity impact loading." *Journal of Mechanics of Materials and Structures*. 4(7-8), pp. 1429-1451. 2009. DOI: 10.2140/jomms.2009.4.1429

[7] Olsson, R. "Impact response of orthotropic composite plates." *AIAA Journal*. 30(6), pp. 1587-1596. 1992. DOI: 10.2514/3.11105

[8] Kiani, Y., Sadighi, M., Jedari Salami, S., Eslami, M. R. "Low velocity impact response of thick FGM beams with general boundary conditions in thermal field." *Composite Structures*. 104, pp. 293-303. 2013. DOI: 10.1016/j.compstruct.2013.05.002

[9] Mao, Y. Q., Fu, Y. M., Chen, C. P., Li, Y. L. "Nonlinear dynamic response for functionally graded shallow spherical shell under low velocity impact in thermal environment." *Applied Mathematical Modelling*. 35(6), pp. 2887-2900. 2011. DOI: 10.1016/j.apm.2010.12.012

[10] Qian, Y., Swanson, S. R. "A comparison of solution techniques for impact response of composite plates." *Composite Structures*. 14(3), pp. 177-192. 1990. DOI: 10.1016/0263-8223(90)90047-i

[11] Efraim, E. "Accurate formula for determination of natural frequencies of FGM plates basing on frequencies of isotropic plates." *Procedia Engineering*. 10, pp. 242-247. 2011. DOI: 10.1016/j.proeng.2011.04.043

[12] Touloukian, Y. S. "*Thermo-physical Properties of High Temperature Solid Materials*." McMillan, New York. 1967.

[13] Reddy, J. N., Chin, C. D. "Thermomechanical analysis of functionally graded cylinders and plates." *Journal of Thermal Stresses*. 21(6), pp. 593-626. 1998. DOI: 10.1080/01495739808956165

[14] Boroujerdy, M. S., Kiani, Y. "Low velocity impact analysis of composite laminated beams subjected to multiple impacts in thermal field." *ZAMM - Journal of Applied Mathematics and Mechanics / Zeitschrift für Angewandte Mathematik und Mechanik*. pp. 1-14. 2015. DOI: 10.1002/zamm.201500132

[15] Jam, J. E., Kiani, Y. "Low velocity impact response of functionally graded carbon nanotube reinforced composite beams in thermal environment." *Composite Structures*. 132, pp. 35-43. 2015. DOI: 10.1016/j.compstruct.2015.04.045